Proposal for the Hall-D Beam Line Pair Spectrometer - Goals, Technical Description, and Specifications

1) Introduction

The photon beam source for Hall-D will be based on coherent bremsstrahlung of the CEBAF 12 GeV beam with a diamond radiator. The photon beam generated by the interaction with the diamond radiator will consist of contributions both of incoherent un-polarized bremsstrahlung photons and partially linearly polarized coherent bremsstrahlung photons. As the angular divergence of the incoherent component is larger than the divergence of the coherent component, the coherent component of the photon beam can be enriched relative to the incoherent component by applying tight collimation after a sufficiently large drift space after the diamond radiator. It is planned to place the primary collimator of 3.4 mm diameter for Hall-D 76 m downstream of the diamond radiator which is roughly 22 m in front of the GlueX detector. This restricts the polar angles to less than ~22 μrad as compared to the characteristic divergence of incoherent bremsstrahlung of $m_e/E_e \approx 42\mu rad$. A tagging spectrometer, referred to as the tagger, will be built 2 m downstream of the radiator and will measure the energy of the electrons which radiated the photons, the photon energy will then determined from energy conservation. The tagger will be readout for every GlueX trigger and will be the primary measurement of the photon energy, but the measured photon flux will be a convolution of the collimated photon spectrum with the trigger efficiency ($I_\gamma^{meas}(E) = I_\gamma^{coll}(E)\varepsilon(E)$). Cross section measurements at GlueX will require a knowledge of the photon spectrum $I_\gamma^{coll}(E)$, that in principle could be determined by the GlueX detector itself from the measured trigger rates. However this would require understanding the acceptance and trigger efficiencies at the 1-2% level. In practice, an additional instrument will be needed for a precise measurement of the photon flux incident on the GlueX target. In addition to the absolute flux measurement, the linear polarization of the photon beam also needs measured.

In order to have a precision measurement of the characteristics of the photon beam it is necessary to base the measurement on a well understood process. It is proposed to use pair production which is a well understood QED process as the basis for the luminosity measurement and polarization determination. The pair production cross section between E_γ of 12 and 6 GeV is accurate to better than 1%. In this document a pair spectrometer is proposed based on a single magnet and a simple detector array. Such a magnet design, with simple field topography, is chosen to minimize the uncertainty of the calculated electron and positron trajectories. The pair spectrometer is self calibrating to the extent that the absolute energy scale can be determined from the high energy edge of the photon spectrum. The endpoint of the spectrum corresponds to the CEBAF beam energy which is known to better than 1 part in 10^{-3}. The beam flux $I_\gamma^{coll}(E)$ is determined from the coincidence rates in the spectrometer. The excellent energy calibration of the pair spectrometer will allow a cross calibration of the photon energy measurement in the tagger spectrometer by looking at coincidences between the two spectrometers. This technique can also be used to determine the tagger trigger efficiency. Finally a careful analysis of the flux function $I_\gamma^{coll}(E)$ can determine the polarization of the photon beam. In summary the goals for this Pair Spectrometer are as follows:

a) Continuously measure the beam flux $I_\gamma^{coll}(E)$ as a function of energy between 6 and 12 GeV.
b) Determine the photon beam linear polarization.
c) Provide an independent tagger energy calibration.
d) Measure the tagger trigger efficiency.

In addition to the above goals the pair spectrometer must be designed so that the spectrometer can be upgraded in the future with silicon pixel detectors to measure the photon beam linear polarization directly. As these detectors must be placed in front of the pair spectrometer magnet and there needs to be enough drift distance between the converter and the pixel detectors to resolve both the polar and azimutal angles of the electrons and positrons.

2) Pair Spectrometer Design

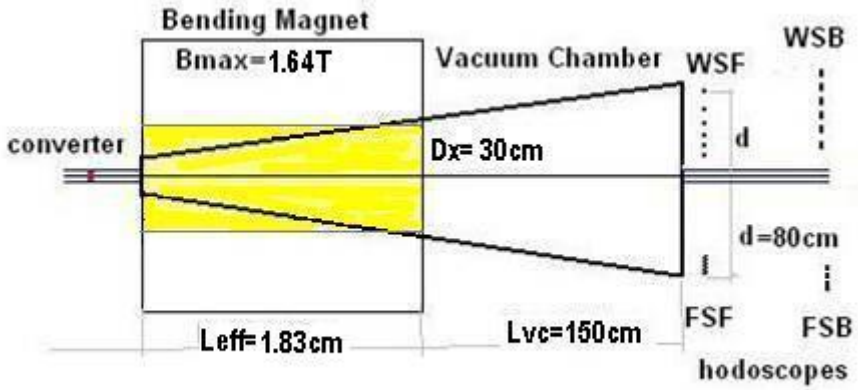

Figure 1 Layout of the proposed pair spectrometer. On the left is a thin 10^{-4} radiation length converter followed by a strong spectrometer magnet. The vacuum chamber extends 1.5 m beyond the end of the magnet. Immediately outside the vacuum chamber is a scintillator hodoscope detector.

The layout of the proposed pair spectrometer is shown in Figure 1. The 6 – 12 GeV photon beam is sampled with a thin converter shown on the left of Figure 1. As the pair production cross section is large, a thin converter can be used. The optimum choice for the converter thickness will depend on the details of the detector design and photon beam flux and will therefore be discussed after the detector is described. The target holder will be positioned at least 1 m upstream of the pair spectrometer magnet and will be equipped with several different thickness radiators. The converter ladder can also be completely removed from the beam.

The beam spot size on the pair spectrometer converter is about 3.4mm in diameter which is much larger than the projection of the opening angles of produced pairs on the spectrometer's detection planes, as the production angle divergence is typically m_e/E_γ = 42 - 85 μrad. Multiple Coulomb scattering angles, assuming converter thickness $10^{-3}X_o$, are on the order of 55-145 μrad. The magnetic field needs to be strong enough because the larger the Int[B*dL] of the magnet the more dispersed the electrons and positrons will be on the hodoscope plane and the better the momentum resolution. The pole needs to be also wide enough because the width of the pole defines the lowest momentum measureable in the spectrometer. A survey of available magnets has been performed and the magnet best suited for our applications selected. This magnet has a pole width of about 600 mm and an effective length of about 1.83 m. The exact numbers can only be determined after plates have been designed to reduce the magnet gap from 150 mm to 25-30mm ($>10\sigma$, where σ -1mm for the beam spot size of 3.4mm). The magnet should operate at a field where the iron is not saturated, so the field will be reproducible at 1 in 10^{-4}. For this study a 1.64 tesla field is assumed. If the magnet is operated at1.63 tesla, electrons/positrons with a momentum of 3.0 GeV have a horizontal displacement at the end of

the magnet of 28 cm, so the pole width of ±30 cm is just sufficient to accept this momentum. The vacuum chamber downstream of the magnet is limited in length to about 1.5 m by space requirements for equipment necessary for the GlueX detector. Given the parameters of the magnet the chamber needs to be 1.6m wide at the downstream end. One necessary condition on the spectrometer design is that 12 GeV electrons or positrons generated in the converter must be able to pass through the exit window at the end of the vacuum chamber and strike a shielding wall. This protects GlueX from unnecessary background. With this design 12 GeV electrons or positrons will exit the vacuum chamber 18 cm from photon beam axis leaving sufficient space for a flange to couple the photon beamline and the exit window mount. The vacuum chamber is constructed of non-magnetic material (aluminum or stainless steel). In summary, a magnet with an effective length L_{eff} = 1.829 m, an integrated field strength Int[B*dL] =2.991 T*m, an operating field B_{max} = 1.64 tesla, and a pole width D_x = ±30 cm is assumed. The vacuum chamber extends 1.5 m beyond the end of the magnet.

The scintillator hodoscope detectors are shown on the right in Figure 1. The Fine Spacing Forward (FSF) hodoscope (positron arm) and Wide Spacing Forward (WSF) hodoscope (electron arm) are used for the energy determination while the Fine Spacing Backward hodoscope (FSB) and Wide Spacing Backward hodoscopes (WSB) are used for triggering purposes. The FSF hodoscope will measure in fine momentum bins between 3 and 4 GeV. The WSF is a sequence of single scintillators at intervals corresponding to 1GeV and covering the range 3.25 to 8.25 GeV. As the spacing between the counters in the WSF hodoscope corresponds

N	momentum p(GeV)	radius of curvature R (m)	Scattering Angle (rad)	Scattering Angle Degrees	Displacement at end of mag. (m)	x drift (m) magnet to hodo	x (m) at hodoscope	Counter width (m)
1	3.0000	6.1018	0.3044	17.4425	0.2806	0.4713	0.7519	0.0111
2	3.0417	6.1865	0.3001	17.1961	0.2765	0.4642	0.7408	0.0108
3	3.0833	6.2713	0.2959	16.9566	0.2726	0.4574	0.7300	0.0104
4	3.1250	6.3560	0.2919	16.7238	0.2688	0.4507	0.7195	0.0101
5	3.1667	6.4408	0.2879	16.4974	0.2652	0.4442	0.7094	0.0099
6	3.2083	6.5255	0.2841	16.2772	0.2616	0.4380	0.6995	0.0096
7	3.2500	6.6103	0.2803	16.0628	0.2581	0.4319	0.6900	0.0093
8	3.2917	6.6950	0.2767	15.8541	0.2547	0.4260	0.6807	0.0091
9	3.3333	6.7798	0.2732	15.6508	0.2514	0.4202	0.6716	0.0088
10	3.3750	6.8645	0.2697	15.4527	0.2481	0.4147	0.6628	0.0086
11	3.4167	6.9493	0.2663	15.2597	0.2450	0.4092	0.6542	0.0083
12	3.4583	7.0340	0.2630	15.0714	0.2420	0.4039	0.6459	0.0081
13	3.5000	7.1187	0.2598	14.8878	0.2390	0.3988	0.6377	0.0079
14	3.5417	7.2035	0.2567	14.7087	0.2361	0.3938	0.6298	0.0077
15	3.5833	7.2882	0.2537	14.5339	0.2332	0.3889	0.6221	0.0075
16	3.6250	7.3730	0.2507	14.3632	0.2305	0.3841	0.6146	0.0073
17	3.6667	7.4577	0.2478	14.1965	0.2278	0.3795	0.6072	0.0072
18	3.7083	7.5425	0.2449	14.0337	0.2251	0.3749	0.6000	0.0070
19	3.7500	7.6272	0.2422	13.8747	0.2225	0.3705	0.5931	0.0068
20	3.7917	7.7120	0.2394	13.7192	0.2200	0.3662	0.5862	0.0067
21	3.8333	7.7967	0.2368	13.5672	0.2176	0.3620	0.5795	0.0065
22	3.8750	7.8815	0.2342	13.4186	0.2152	0.3579	0.5730	0.0064
23	3.9167	7.9662	0.2317	13.2732	0.2128	0.3538	0.5667	0.0062
24	3.9583	8.0510	0.2292	13.1310	0.2105	0.3499	0.5604	0.0061
25	4.0000	8.1357	0.2267	12.9918	0.2083	0.3461	0.5543	
					Total width of the FSF hodoscope			0.19753

Table 1: Detailed summary of the fine spaced forward (FSF) hodoscope. In this design 41.7 MeV/c momentum bins are used. The radius of curvature in the magnet, the bend angle in the magnet, the x-displacement at the end of the magnet, and the x-coordinate at the hodoscope are computed for the momentum corresponding to the edge of every momentum bin. The counter widths are computed in the right column.

to the total range of coverage in the FSF every momentum bin from 12.25 GeV to 6.25 GeV corresponds to a coincidence between only one pair of scintillators. This spectrometer design provides uniform acceptance over the energy range of 12.4 GeV to 6.4 GeV using a minimum number of counters and readout channels. The disadvantage of this design is that the overall acceptance for the produced pairs is low, that is the cost for the fine photon energy resolution. Cross sections, rates, and acceptance will be discussed in the performance section.

The FSF hodoscope is a single layer close packed scintillator hodoscope with fine segmentation covering the momentum range between 3 and 4 GeV. The FSF hodoscope will consist of 24 scintillator counters each with a momentum acceptance of 1 GeV/24 = 41.7 MeV. A constant momentum acceptance per channel requires adjusting the width of each counter. Table 1 summarizes the important parameters for the positrons with momentum such that they strike the boundaries between the individual counters in the FSF. This information defines the design of the FSF. For every momentum bin the curvature in the magnet was computed and the scattering angle and displacement at the exit of the magnet determined. Using the scattering angle, the horizontal displacement due to the 1.5 m long drift space is computed and finally the horizontal position of the particles on the hodoscope. The hodoscope is 19.75 cm wide and the width of the individual counters range from 6.6 to 11.1 mm. Table 2 summarizes the design of the FSF. The momentum range, uncertainty, position and width of each counter are listed. With this design the high momentum counter has a width of 6mm which is roughly twice the photon beam spot size on the converter. The effect of the beam spot size on the detector resolution was estimated by modifying the FSF strip width making it the quadratic sum of the beam spot size and the sizes shown in Table2. The size of the effect was found to be 7 to 12% for a 24 channel FST. A careful MC study of the detector resolution taking into account the spot size, multiple scattering, and the pair production opening angle needs to be performed to exactly determine the optimum number of counters but it is clear this design is close to the optimum. Another important factor to be considered when selecting the momentum binning of the FSF is the impact this binning has on the ability to determine the polarization of the photon beam by fitting the shape of the photon energy spectrum. The number of energy bins per GeV needs to be selected fine enough so that

Counter	Momentum bin Minimum GeV/c	Momentum bin Maximum GeV/c	Momentum bin width MeV/c	Momentum Uncertainty mm ΔE/√12	X-coord. of Scintillator m	Scintillator width mm
1	3.0000	3.0417	41.6667	12.0281	0.7519	11.1038
2	3.0417	3.0833	41.6667	12.0281	0.7408	10.7690
3	3.0833	3.1250	41.6667	12.0281	0.7300	10.4495
4	3.1250	3.1667	41.6667	12.0281	0.7195	10.1446
5	3.1667	3.2083	41.6667	12.0281	0.7094	9.8532
6	3.2083	3.2500	41.6667	12.0281	0.6995	9.5745
7	3.2500	3.2917	41.6667	12.0281	0.6900	9.3079
8	3.2917	3.3333	41.6667	12.0281	0.6807	9.0525
9	3.3333	3.3750	41.6667	12.0281	0.6716	8.8078
10	3.3750	3.4167	41.6667	12.0281	0.6628	8.5731
11	3.4167	3.4583	41.6667	12.0281	0.6542	8.3480
12	3.4583	3.5000	41.6667	12.0281	0.6459	8.1318
13	3.5000	3.5417	41.6667	12.0281	0.6377	7.9241
14	3.5417	3.5833	41.6667	12.0281	0.6298	7.7245
15	3.5833	3.6250	41.6667	12.0281	0.6221	7.5325
16	3.6250	3.6667	41.6667	12.0281	0.6146	7.3478
17	3.6667	3.7083	41.6667	12.0281	0.6072	7.1699
18	3.7083	3.7500	41.6667	12.0281	0.6000	6.9985
19	3.7500	3.7917	41.6667	12.0281	0.5931	6.8334
20	3.7917	3.8333	41.6667	12.0281	0.5862	6.6741
21	3.8333	3.8750	41.6667	12.0281	0.5795	6.5205
22	3.8750	3.9167	41.6667	12.0281	0.5730	6.3722
23	3.9167	3.9583	41.6667	12.0281	0.5667	6.2291
24	3.9583	4.0000	41.6667	12.0281	0.5604	6.0908

Table 2: Summary of the FSF hodoscope design. The momentum range, momentum uncertainty, position, and size for each counter are shown.

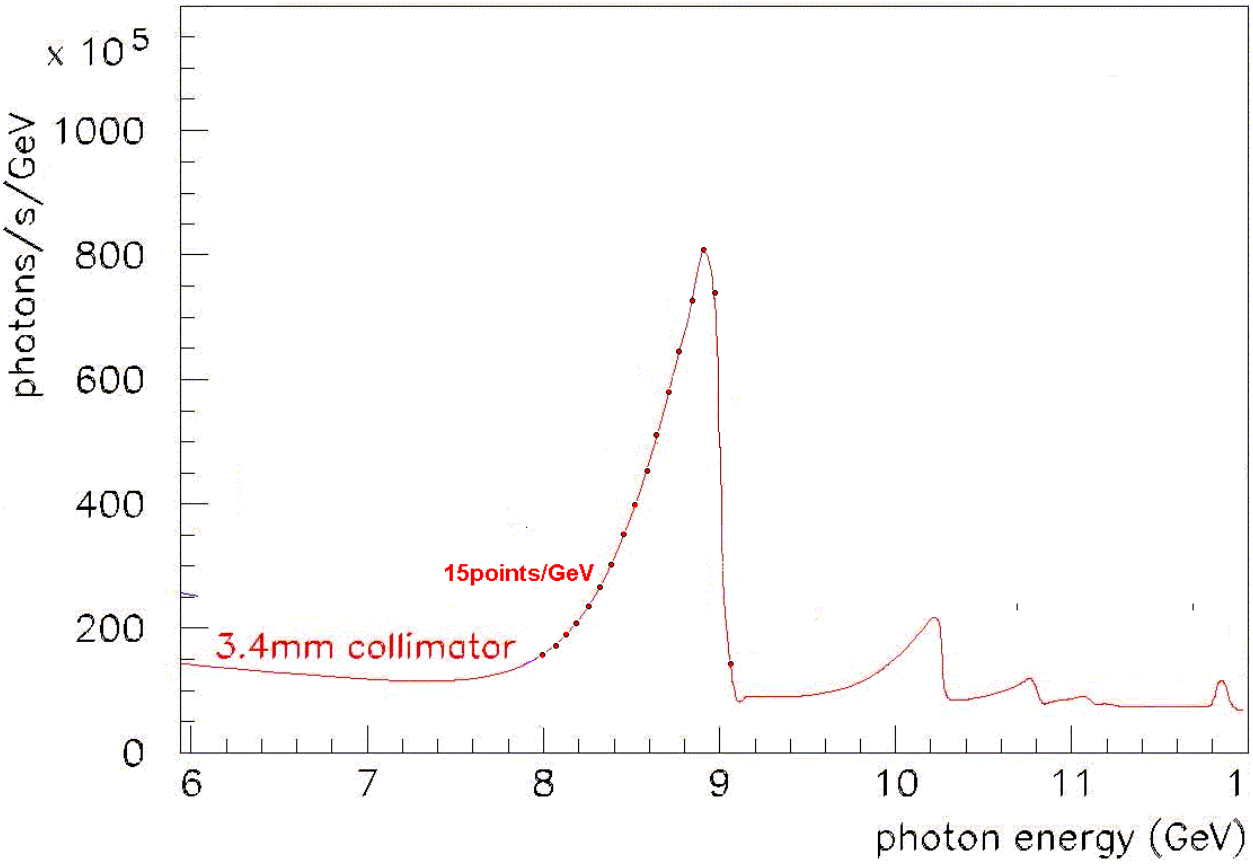

Figure 2 A typical photon energy spectrum is shown for a 3.4mm collimator. Superimposed on the curve are the energy measurement points corresponding to a FSF hodoscope with 15 scintillators.

the corresponding uncertainty in the fit to the coherent bremsstrahlung spectrum does not dominate the uncertainty in the determination of the linear polarization. As was evaluated from Figure 2, already 15 bins per GeV gives a fairly accurate determination of the shape, while in the present design 24bins/GeV is considered. As part of the MC studies the impact of changing the binning on the uncertainty in the linear polarization measurement should be studied.

The WSF hodoscope is a set of six narrow scintillators positioned to detect electrons in steps of 1GeV/c ranging from 3.25 to 8.25 GeV/c. The 3.25 GeV/c lower limit for the WSF hodoscope is determined by the width of the magnet poles; a 2.25 GeV/c particle will not pass through the magnet. Signals from the two detector arms are taken in coincidence and the photon energy is the sum of the positron and electron energies, so this combination of detectors then covers the momentum range of 6.25 to 12.21 GeV/c. As the FSF and the WSF measure the positron and electron energies independently, the uncertainty in the photon energy is the sum of the energies of the electron and positron added in quadrature. The equation for the photon energy uncertainty is then:

$$\sigma_\gamma = (\sigma_+^2 + \sigma_-^2)^{1/2}$$

where σ_γ is the uncertainty in the photon energy and σ_+ and σ_- are the uncertainties in the positron and electron energies respectively. Correspondingly, the equation for the energy resolution using the relation $E_\gamma = E_- + E_+$ is:

$$(\sigma_\gamma / E_\gamma) = (\sigma_+^2 + \sigma_-^2)^{1/2} / (E_- + E_+).$$

It is clear from the above equations that once the segmentation and therefore the resolution of the FSF has been chosen the optimum design of the WSF is highly constrained. The WSF scintillator widths should be chosen so that the overall photon energy uncertainty is not dominated by the WSF. Reducing the counter widths much below what is needed to match the FSF resolution would needlessly reduce the spectrometer acceptance. In this design the widths of the WSF scintillators was adjusted such that the uncertainty in the photon energy is constant for all combinations of FSF and WSF counter pairs. The width of the WSF counters were chosen so that the uncertainty in the reconstructed photon energy was equal to ½ the momentum bin width in the FSF or 20.8 MeV,

$$\sigma_\gamma = \text{(FST momentum bin width)}/2 = 20.8 \text{ MeV}.$$

As the uncertainty in momentum measurement in the FSF counter is 12 MeV, this requires that the uncertainty in the momentum from the WST is 17 MeV. In Table 3 the most important parameter of the WSF hodoscope are summarized. The widths of the counter needed to measure the momentum with an accuracy of 17 MeV varies from 1.3 cm at 3.25 GeV to 0.2 cm at 8.25 GeV. By designing the spectrometer so that the photon energy resolution is equal to ½ the FST momentum bin width, adjacent photon energy measurement points are separated by an amount equal to the uncertainty in the measurement. This avoids any strong overlap between neighboring photon energy measurement points.

Counters of WSF hodoscope	P GeV/c	Electron bending angle deg	Radius of curvature M	Distance to beam line Cm	Scintillator width for σ_γ=21.7MeV cm
WSF1	3.25	16.03	6.62	68.8	1.31
WSF2	4.25	12.19	8.66	51.9	0.75
WSF3	5.25	9.84	10.69	45.4	0.54
WSF4	6.25	8,25	12.75	35.0	0.35
WSF5	7.25	7.11	14.78	30.1	0.25
WSF6	8.25	6.24	16.83	26.4	0.2

Table 3: Detailed summary of the wide spaced forward (WFS) hodoscope detectors.

Looking at the widths of the strips in the WSF arm shown in Table 3 column 6, one sees that the width of the counters decreases as the momentum increases. This is necessary to match the momentum spread in the WSF to the photon energy resolution given the fixed resolution in the FSF arm.

E_γ range*GeV)	6-7	7-8	8-9	9-10	10-11	11-12
Widths of WSF strips convoluted with beam spot size.(cm)	1.353	0.82	0.64	0.49	0.42	0.4
σ_γ(corrected) (MeV)	23.2	24.0	25.5	28.7	32.2	38.1

Table4. Summary on WSF strips' effective width (beam spot size convoluted) and impact to a photon energy resolution. The FSF resolution affected by beam spot size is set to 13MeV/c.

Monoenergetic particles produced in the converter do not image to a point on the hodoscope plane due to the several factors, mainly by the beam spot size of 3.4 mm on the radiator, but also multiple scattering in the radiator and the small transverse momentum spread in the pair production process also contribute. The impact of the beam spot size to the photon energy resolution is estimated by computing an "effective" WSF strips widths size. This effective strip width is computed as a square root of the quadratic sum. From this strip width the effective momentum uncertainty in the WSF and the photon energy uncertainty are computed. The results are shown in Table 3. This effect of the position spread nearly doubles the error in the photon energy measurement in the large energy bins. The uncertainty is increased from 21 MeV to 38 MeV for photons between 11 and 12 GeV. In the region of the peak of the coherent bremsstrahlung (P- = 5.25GeV and P_+ ranges between 3 and 3.96GeV) the effect of the beam spot size on the energy resolution is 18% (25.5 MeV instead of 21.7MeV).

The details of backward layer hodoscopes are not presented here because the studies to understand if they are needed are still underway and will depend on background rate estimates. However similar trigger hodoscopes are in use in the Hall-B pair spectrometer and are important to suppress the noisy background. Their need in the Hall-D pair spectrometer may be also be indirectly confirmed from Hall B's data on single arm and coincidence rates. The geometry of the backward layer hodoscopes is shown in the layout above and is used for the design of the trigger scheme presented below. The present backward hodoscopes consist of 6 strips behind the WSF hodoscope and 3 strips behind the FSF hodoscopes. The trigger hodoscope arrays are located 1m downstream of the WSF (6) and FSF (16) hodoscopes.

3) Pair spectrometer projected performance

a) Energy resolution, efficiency, and rates

The pair spectrometer energy resolutions for FSF granularities of 16 and 24 channels after correcting for the beam spot-size are summarized in Table 3.

	E_γ = 8-9 GeV		E_γ= 11-12GeV	
	n=16	n=24	n=16	n=24
σ_γ(MeV)	35.6	25.5	45.8	38.1

Table 5: The uncertainty in the reconstructed photon energy is shown depending on whether the FSF is constructed of n=16 of 24 counters. The uncertainty is shown for both the coherent bremsstrahlung region (8-9 GeV) and the high energy bins.

There is a noticeable gain in photon resolution below 10GeV for FSF granularity n=24 while at the high energy end of the bremsstrahlung spectrum the beam spot size has a larger effect and so the improvement in resolution is smaller. If one increase the widths of WSF counters 5 and 6 to 0.4cm in order to increase the acceptance and therefore count rate, the photon energy resolutions become 51.7 and 49.5 MeV for n=16 and 24 bins respectively. Detailed studies of the rate as a function of radiator thickness will be performed to determine if the 2 mm counters are acceptable.

The efficiency for each photon energy bin is defined by a two arm coincidence and has to be accurately determined. The relative efficiency of each pair spectrometer channel can be directly

measured using a bremsstrahlung spectrum that has a known shape. An amorphous radiator installed in the goniometer will provide a collimated purely incoherent energy spectrum from which the relative efficiency for each channel can be determined by comparing the measured and calculated energy spectrum. This procedure should be regularly repeated in order to monitor and correct any possible instability. The absolute efficiency of the pair spectrometer can be measured experimentally at a known but small flux using a total absorption counter.

The rates in the pair spectrometer were evaluated as the product of the momentum phase space coverage in both arms at a few photon energies. The acceptance was found to be approximately 0.1%/GeV on average, decreasing toward the high energy end of the bremsstrahlung spectrum (0.15% at 6GeV, 0.1% at 9GeV and 0.08% at 12GeV). With this acceptance and assuming 100% detector efficiency, the expected rate in the region of the coherent bremsstrahlung peak is on the order of 100 Hz for a converter thickness of ~10^{-3} radiation lengths and a photon flux of ~10^{8} photons/s.

The absolute energy scale for the pair spectrometer can be measured by accurately determining the endpoint of the bremsstrahlung spectrum. The endpoint of the spectrum corresponds to the CEBAF beam energy which is known to better than 1 part in 10^{3}. Measuring the endpoint of the bremsstrahlung spectrum then determines the absolute energy scale up to the resolution of the pair spectrometer. A resolution of about 42 MeV is expected at 12 GeV, but the endpoint energy uncertainty extracted by the fit will be much less if statistically ensured.

The overall error on the photon energy measurement will depend on the accuracy of the scintillator dimensions, the placement accuracy of the scintillators, the precision of the field map, multiple scattering in the converter, uncertainty in the bremsstrahlung process itself, and the beam spot size on the converter. Each of the contributions to the error will need to be studied in detail.

b) Tagger calibration

As an instrument with simple configuration the energy of the photons can accurately be determined using the pair spectrometer (PS). Therefore it can be used as a reference to cross calibrate the tagger spectrometer which has more complicated configuration and operates at a

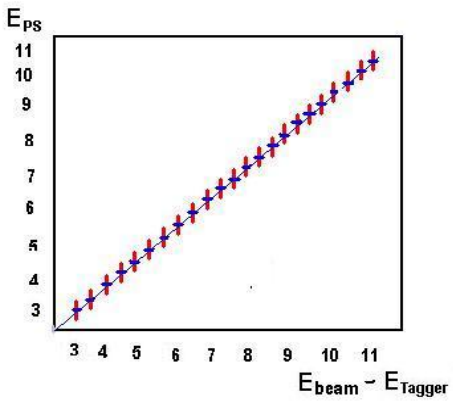

Figure 3: Cross calibration of the tagger using the pair

much higher rate (>10^{11}). The tagger spectrometer measures the energy of the photons in the beam by measuring the energy of the scattered electrons and the pair spectrometer measures the energy of a small fraction of these photons which undergo pair production in the PS radiator. By looking at the events where a coincidence exists between the tagger and the pair spectrometer these two energy measurements can be compared. A typical cross-check of the photon energy measured in the PS and the tagger is shown in a scatter-plot in Figure 3. Each point in the plot is the combination of PS and tagger measurement. The error bars on the plot correspond to the energy resolutions for the PS and tagger in each energy bin. In this plot the energy resolution of the tagger is higher than that of the PS but this does not affect the precision of the cross-check as enough statistics can be collected to make the uncertainty in the mean of the distributions arbitrarily small. Random coincidences between the tagger and pair spectrometer could shift the calibration curve so care needs to be taken in the analysis.

c) Photon beam linear polarization determination

Careful analysis of the shape of the coherent bremsstrahlung spectrum allows one to determine the linear polarization of the photon beam. The methods developed for this task are quite advanced and require precise data over a wide enough energy range above and below the peak region [1][2]. For example, at if the coherent bremsstrahlung peak is at 9 GeV, the range from 6 to 12 GeV is quite appropriate for this task. The expected precision will be on the order of 0.01-0.02 over the working range of $(E-E_{peak})/ E_{peak}<0.3$. Outside of this range the polarization is low and compatible with zero.

d) Electronics

The entire pair spectrometer consist of a total of 42 counters: FSF(24),FSB(4),WSF(6),and WSB(6). The original proposed readout and trigger schemes for the detector are shown in Figures 4. In Figures 5 and 6 the implementation of this scheme in GlueX standard electronics is presented. The scintillators are read out using photomultiplier tubes which are powered by a CAEN SY2527 based high voltage system. The signals from the FSF and WSF are discriminated using CAEN V812 constant fraction discriminators and then readout using the F1TDC. The backward layer hodoscopes are used to form the pair spectrometer trigger and are readout with the fADC250 operating in “HIT BIT Mode”. A bit pattern containing the information as to which of the back hodoscope channels was hit is formed in the fADC250 and passed to the crate trigger processor (CTP). The CTP passes this information to the subsystem processor (SSP) and the SSP passes it to the global trigger processor (GTP). The GTP checks for coincidences between the WSB and FSB hodoscopes and generates a pair spectrometer trigger if one is found.

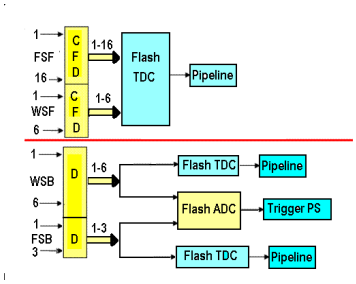

Figure 4: Sketch of the original proposed electronics.

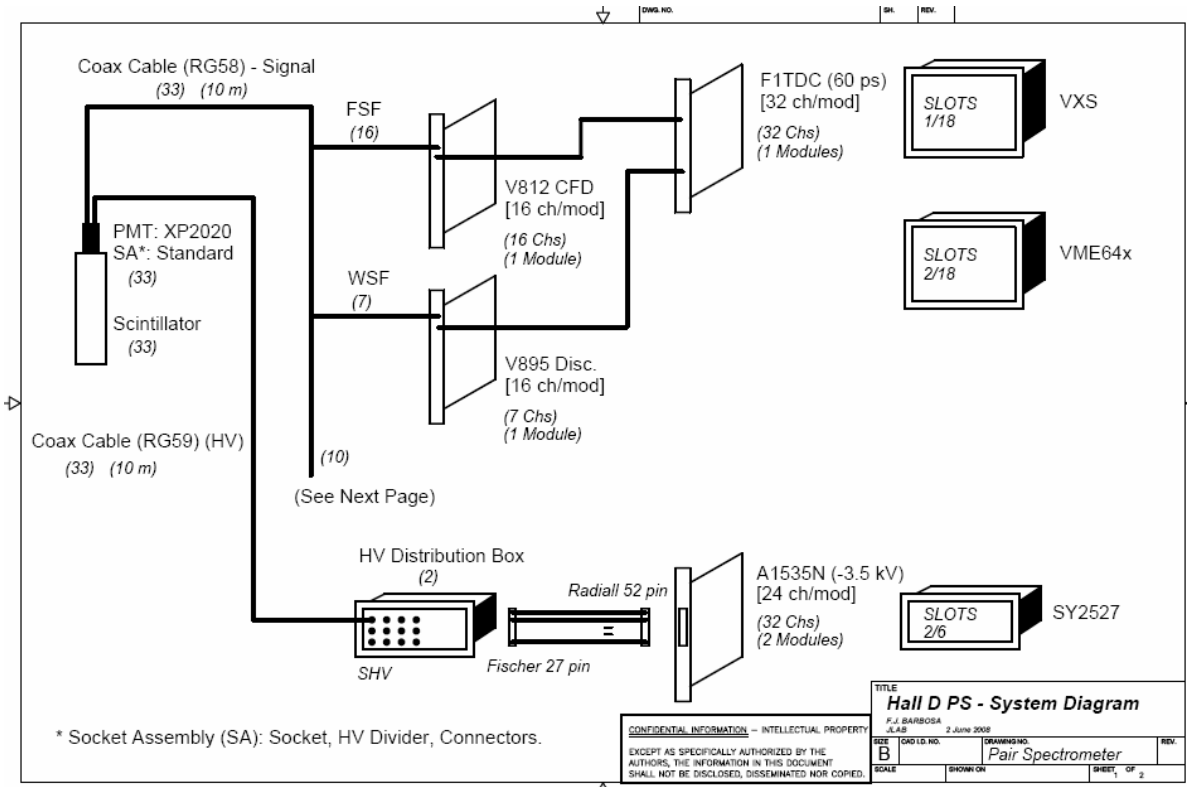

Figure 5: Readout scheme for the pair spectrometer.

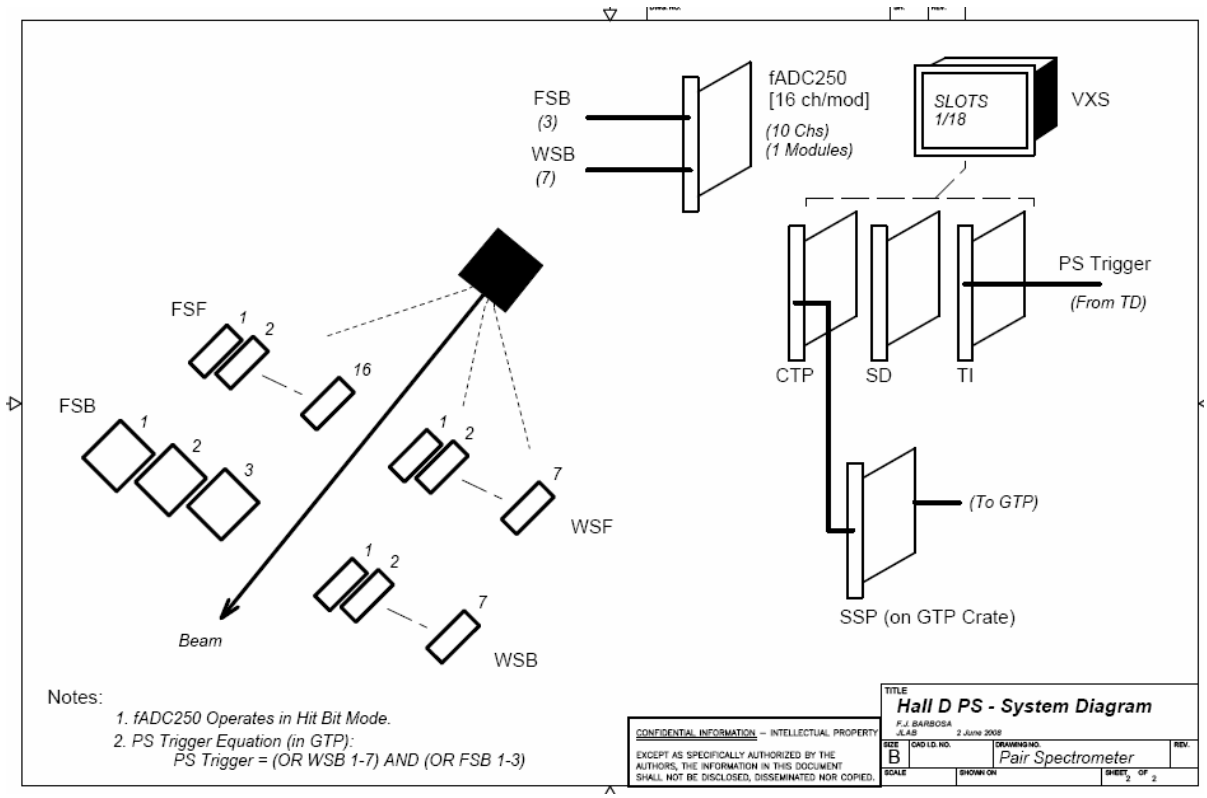

Figure 6: Trigger scheme for the pair spectrometer

e) Software

A large amount of software will be needed to operate the SP and analyze the data. The major software packages include:

- The software needed to measure the channel by channel efficiency of the PS using the incoherent bremsstrahlung spectra.
- Software to search for the crystal axes orientation in the radiator using angular scan information.
- Online software to measure and monitor the coherent bremsstrahlung spectra and provide feedback information for the radiator crystal positioning.
- Off-line pair spectrometer data analysis and coherent bremsstrahlung polarization calculations.

All these programs were developed for YERPHI's γ-2 linearly polarized beam facility and can be adopted to Hall D's special requirements and conditions .

f) Work to do: First steps

1. To look for the best dipole magnet available for the spectrometer.
2. Once the magnet is decided on precise trajectory calculations need to be performed to determine the optimum detector layout using that magnet field topography.
3. A full simulation of the pair production process for 6-12 GeV photons using the selected PS layout needs to be performed to determine the resolutions and efficiencies.
4. The counter structure needs selected: scintillator type, light guides, PMT's.
5. The PS detector mechanical infrastructure must be designed: hodoscope counter construction including mounts and magnetic shielding, movable supports and rails for precise adjustments of the counters to relevant coordinate references.
6. Design and prototyping of the counters with special attention to quality control issues. Preparation of the test benches for certification of hodoscopes and counters after assembly.

The Yerivan group is able to do these steps.

[1] Tubingen Group Paper(will find…)
[2] S.Darbinyan, H.Hakobyan,R.Jones, A.Sirunyan and H.Vartapetian , NIM A554(2005)75-84